Int. J. Plant Bas. Pharm. (2022) 2(2), 239-251

INTERNATIONAL JOURNAL OF PLANT BASED PHARMACEUTICALS

https://ijpbp.com

RESEARCH ARTICLE

OPEN ACCESS

Morphology, biological and chemical profiling of three *Polyscias* species, endemic to Mauritius

Minu Gupta Bhowon[a,*], Lee Suan Chua[b], Shobha Jawaheer[c], Ayeshna D. Soodhowa[a], Sabina Jhaumeer Laulloo[a,*]

[a] *University of Mauritius, Faculty of Science, Department of Chemistry, Réduit 80837, Republic of Mauritius*
[b] *Universiti Teknologi Malaysia, Institute of Bioproduct Development, Johor Bahru, 81310 UTM Skudai, Malaysia*
[c] *University of Mauritius, Faculty of Science, Department of Biosciences and Ocean Studies, Réduit 80837, Republic of Mauritius*

ARTICLE INFO

Article History:

Received: 17 June 2022
Revised: 02 July 2022
Accepted: 30 July 2022
Available online: 03 August 2022

Edited by: B. Tepe

Keywords:
Polyscias
Anatomy
Morphology
Phytochemicals
Antioxidant
Anti-glucosidase

ABSTRACT

The aim of the study is to screen the morphological, anatomical, biological, and chemical profiles of the leave extracts of endemic *Polyscias* species namely *P. dichroostachya* (PD), *P. gracilis* (PG), and *P. mauritiana* (PM) from Mauritius. The morphology and anatomy of the leaves were studied using a microscope. Phytochemical screening of extracts using LC-MS/MS was carried out by ionization in both positive and negative modes. The leaves are pinnately compound, hypostomatic, dorsiventral, with a prominent mid vein with secretion cavities, and they can be distinguished by their midrib shape and anatomy. From the molecular mass and fragmentation data, 31 terpenoid saponins, 19 flavonoids, 17 acids, 7 terpenes, and 10 miscellaneous compounds including pyrrolidines and acetylenes in different extracts (hexane, ethanol, and aqueous) were identified. Extracts from the three species using DPPH radical scavenging activity exhibited good to moderate antioxidant activities with IC_{50} values in the range of 2.1-70.8 mg/ml and the ethanolic extract of PD showing the highest activity. Aqueous extracts of PG and PM potently inhibited alpha-glucosidase with IC_{50} values of 0.50 and 2.62 mg/ml. The different leaf extracts exhibited moderate activity against a panel of gram-positive and gram-negative bacteria. This is probably the first report on the extensive chemical profiling and morphology of these endemic *Polysias* spp. from Mauritius and the results indicate that these leaf extracts have beneficial health properties and are thus worth exploiting further.

1. Introduction

The rise in the incidence of diseases together with extensive resistance to existing drugs calls for a continuous quest for new drugs. During the past decades, there has been ongoing drug discovery research, which requires a constantly expanding library of compounds with a wide range of molecular and chemical diversity. Natural products chemistry is considered to be a principal area of research at the interface of chemistry and biology which involves the isolation and characterization of novel bioactive compounds.

Mauritius with an area of 1,865 km^2 is a volcanic island in the Indian Ocean (20°S, 57°E) with a rich botanical diversity consisting of around 700 native species of flowering plants of which 39.5 % are strictly endemic (Baider et al., 2010). This relatively high endemism of Mauritian flora provides a plethora of unique and structurally diverse phytochemicals. However, only a small percentage of the Mauritian endemic plants have been exploited for their medicinal values let alone converted into drug formulation. The Mauritian population has a long tradition of the use of the herbal remedy in the form of "tisanes" or balms to treat diverse ailments such as diabetes, hypertension, gastrointestinal disorders, rheumatism, kidney stones, and anemia, though most of the endemic plants lack phytotherapeutic and scientific evidence to support their medicinal values. There are several scientific reports on the therapeutic potential of endemic plants in Mauritius (Rummun et al., 2018) yet there are only a few studies on the identification of the phytochemicals present in the plants (Świątek et al., 2021). We believe that a substantial fraction of Mauritius native flora resources remain untapped in terms of identification of the metabolites.

* Corresponding author:
E-mail address: sabina@uom.ac.mu (S.J. Laulloo), mbhowon@uom.ac.mu (M.G. Bhowon)
e-ISSN: 2791-7509
doi: https://doi.org/10.29228/ijpbp.6

Please cite this article as: Bhowon, M.G, Chua, L.S., Jawaheer, S., Soodhowa, A.D., Laulloo, S.J., 2022. Morphology, biological and chemical profiling of three Polyscias species, endemic to Mauritius. International Journal of Plant Based Pharmaceuticals, 2(2), 239-251, https://doi.org/10.29228/ijpbp.6.

Polyscias, one of the members of the Araliaceae family, consists of approximately 159 species distributed worldwide. There are several scientific reports on the therapeutic potential of various *Polyscias* spp. where several classes of compounds such as terpenes, terpenoids, and terpenoids saponins have been isolated (Ashmawya et al., 2019). Extracts from these *Polyscias* spp. were found to exhibit multiple biological activities such as antibacterial, antifungal, molluscicidal, anti-asthmatic, wound healing, tyrosine kinase inhibitory, immune-stimulant agent (Ashmawya et al., 2020) and hypoglycemic (Luyen et al., 2018). Fifteen species are found in the Mascarene Islands of which six are endemic to Mauritius namely, *P. dichroostachya*, *P. gracilis*, *P. mauritiana*, *P. maraisiana*, *P. neraudiana*, and *P. paniculata*. To the best of our knowledge, the morphoanatomical and phytochemical profiling of these Mauritian *Polyscias* species remains poorly explored. There is one report where four saponins derivatives were identified from the leaves of *P. dichroostachya* (Gopalsamy et al., 1990).

In light of the above, the present study aims at providing morphological, anatomical, biological, and phytochemical profiles of the leaves of the three endemic *Polyscias* species, *P. dichroostachya* (PD), *P. gracilis* (PG), and *P. mauritiana* (PM) of Mauritius.

2. Materials and methods

2.1. Sampling of plant material

Samples of the three endemic *Polyscias* species were collected, identified, preserved, and vouchered at the Mauritius herbarium, Mauritius Sugarcane Industry Research Institute (MSIRI), Réduit. PM (MAU 0005163) leaves were collected from the Black River Gorges National Park (200 26' 14'' S and 570 28' 30'' E), and PD (MAU 0005163) and PG (MAU 0025780) leaves were collected from the MSIRI, Réduit (200 14' 17 ''S and 570 29' 44'' E, and 200 14' 18'' S and 570 29' 45'' E, respectively) (Figure 1), all during the mid-summer season. Fresh mature leaf samples were used for morphological and anatomical studies.

Figure 1. Sites where leaves were collected

2.2. Leaf characterisation

2.2.1. Leaf morphology

The leaf size was measured and the leaf shape was determined using descriptors by Harris and Harris (1994), namely leaf arrangement, venation, size, shape, and attachment.

2.2.2. Leaf Anatomy

2.2.2.1. Stomata

Epidermal impressions of leaves were prepared using clear nail varnish. The film was removed with sticky tape and placed on microscope slides for the determination of stomatal density using an inverted contrasting microscope (Leica DM IL) equipped with an integrated camera, at a magnification of x400. The number of stomata per unit area (mm^{-2}) and length of closed stomata were determined from the images.

2.2.2.2. Transverse sections of leaves

Fresh leaf samples were fixed by placing 1 x 1 cm pieces of leaf tissue excised from the midrib and lamina region in formaldehyde alcohol acetic acid (FAA) (Stasolla and Yeung, 2015) at 4 °C in a refrigerator overnight. The tissues were dehydrated in a graded series of TBA (*t*-butyl alcohol) solutions (six) for 30 minutes each at room temperature. The solutions were made up of 50 ml water, 40 ml 95% ethanol, and 10 ml TBA; 30 ml water, 50 ml 95% ethanol, and 20 ml TBA; 15 ml water, 50 ml 95% ethanol, 35 ml TBA; 45 ml 95% ethanol, 55 ml TBA; 25 ml 100% ethanol, 75 ml TBA; and 100 ml 100% TBA, respectively. Finally, the plant samples were placed in xylene for 30 minutes before being infiltrated in paraffin. Plant sections were cut at an angle of 7 degrees and thickness of 15 µM using a microtome. They were stained with Safranin O (1% w/v) and Fast Green FCF (0.1% w/v) and viewed using an inverted contrasting microscope equipped with a camera (Leica DM IL). The thickness of the midrib was calculated from the images.

2.3. Chemicals and equipment

L-ascorbic acid was purchased from Loba Chemie, India. Diphenyl-2-picrylhydrazyl (DPPH), phosphate buffer, acarbose, and *p*-nitrophenyl-α-D-glucopyranoside (pNPG) were purchased from Sigma Aldrich, England. Broth and Mueller Hinton agar were purchased from Himedia, India. ^{1}H and ^{13}C NMR spectra were recorded at 250 and 62.9 MHz on a Bruker electro-spin NMR spectrometer. DNM-9602 Microplate Reader was used for antioxidant and anti-glucosidase activities.

2.4. Extraction

The air-dried and powdered leaves (100 g) of each species were extracted with *n*-hexane (250 ml) followed by ethanol (250 ml) at room temperature. The respective solvents were concentrated at 50 °C under reduced pressure. For crude aqueous extracts, powdered leaves (20 g) were soaked in boiling water (150 ml) for 24 h, and the filtrate obtained was freeze-dried.

2.4.1. Yields (%)

PM-Hex: 0.8, PM-Et: 2.1, PM-Aq: 0.7
PG-Hex: 0.5, PG-Et: 6.0, PG-Aq: 1.7
PD-Hex: 0.3, PD-Et: 4.0, PD-Aq: 4.2

2.5. Nuclear magnetic resonance and liquid chromatography with tandem mass spectrometry

The ^{1}H and ^{13}C NMR spectra of the different extracts (*n*-hexane, EtOH, aqueous) were recorded at 250 and 62.9 MHz on a Bruker electro spin NMR spectrometer using $CHCl_3$/DMSO/D_2O as solvents.

An HPLC system (Ultimate 3000, Dionex Corporation, Sunnyvale, USA) was integrated with a quadrupole time-of-flight mass analyzer as the detector. A C18 reversed-phase column (XSelect HSS T3 XP, 2.1 mm × 100 mm × 2.5 µM) was used to separate compounds at a flow rate of 0.15 ml/min. The mobile phase consisted of acidified water with 0.1% formic acid (A) and acetonitrile (B). The gradient of the mobile phase was 0-10 min, 10% B; 10-15 min, 10%-90% B; 15-20 min, 90% B; 20-22 min, 90%-10% B; and 22-30 min, 10% B. All samples (1 mg/ml) were reconstituted in 50% aqueous methanol and filtered through a 0.2 µM nylon filter before injection. The sample injection volume was 5 µl. The sample flowed into the mass analyzer and was ionized for detection. The mass ranged from m/z 100-2000 and was set for compound screening using both positive and negative ion modes with two dependent product ion scans using rolling collision energy. Nitrogen gas was used as a nebulizing (40 psi) and curtain (20 psi) gas. The voltage of the ion spray was set at 5500 V and 4500 V for the positive and negative ion modes, respectively. The declustering and the focusing potentials were set at 40 and 300 V, respectively.

2.6. Antibacterial activity

Cultures of gram-positive bacteria, *Staphylococcus aureus* (ATCC 25923) and *Bacillus cereus* (ATCC 10816), and gram-negative bacteria namely *Escherichia coli* (ATCC 22922), *Klebsiella pneumoniae* (ATCC 13883), and *Pseudomonas aeruginosa* (ATCC 27853), were used to evaluate the antibacterial activity of the different extracts using disc diffusion method. The bacteria were streaked on the Mueller Hinton Agar plate using sterile cotton swabs and 10 µl of the sample (400 mg/ml in DMSO) were placed on paper discs (6 mm). Erythromycin was used as the positive control and DMSO as the negative control. All the plates were incubated at 37 °C for 24 h. The activity was determined by measuring the zone of inhibition in millimetres (mm).

2.7. DPPH radical scavenging assay

The *n*-hexane and ethanol extracts were dissolved in DMSO and the water extracts were diluted in water to obtain a solution of 100 mg/ml. DPPH radical scavenging activity was measured at an absorbance of 492 nm (Laulloo et al., 2018). All tests were done in triplicate and ascorbic acid was used as the positive control.

The percentage of radical scavenging inhibition was calculated using the formula:

$$\%\ Inhibition = \frac{\mathrm{A0} - \mathrm{As}}{\mathrm{A0}}\ x\ 100$$

Where A_0 is the absorbance of the blank and A_s is the absorbance of the sample.

2.8. Anti-glucosidase activity

The anti-glucosidase activity assay was carried out on the aqueous extract of all three species. The extracts were diluted to make a stock solution of 5 mg/ml. Two-fold serial dilutions were carried out to obtain concentrations ranging from 1.25 to 0.02 mg/ml. A mixture of 50 µl buffer, 50 µl test sample, and 50 µl α-glucosidase were placed in a 96-well Elisa plate. The mixture was incubated at 37 °C for 5 minutes and 50 µl of pNPG was added followed by incubation for 15 minutes. The absorbance was read at 405 nm (Joondan et al., 2019). The test was carried out in duplicate and acarbose was used as the positive control.

The percentage of anti-glucosidase inhibition was calculated by:

$$\%\ Inhibition = \frac{\mathrm{A0} - \mathrm{As}}{\mathrm{A0}}\ x\ 100$$

Where A_0 is the absorbance of the blank and A_s is the absorbance of the sample.

A_s = *absorbance of sample - absorbance produced by blank*

3. Results and discussion

3.1. Leaf characterization

PD, PG, and PM are perennial eudicot plants. The morphological, and anatomical studies for each species were carried out only on a few leaves collected from one tree as these three endemic plants are endangered.

3.1.1. Morphology

The leaves of the three species are odd-pinnate (Figure 2) and the laminae of leaflets are net-veined and traversed by a prominent midvein. The leaves of PD are composed of nine leaflets while those of PG and PM is composed of seven and five leaflets, respectively. Mature leaflets of PD were around 16-22 cm long and 7-9 cm wide, elliptic, apices cuspidate, leaf margins undulate, and leaf attachment petiolate. Mature leaflets of PG were around 13-15 cm long and 7-10 cm wide, obcordate, leaf margins undulate, and leaf attachment petiolate while PM was around 17-20 cm long and 12-14 cm wide, elliptic with bent cuspidate apices, and sessile.

Leaf morphology is determined by both the genetic makeup and environmental cues (Fritz et al., 2018). Leaves have to adapt to their environment to optimize gas exchange and light capture for photosynthesis. Leaves from PD and PG were collected from the Mauritius Sugarcane Industry Research Institute (MSIRI), Réduit, at an altitude of about 317 meters above sea level, and were therefore subjected to similar environmental conditions with little competition. The PM leaves on the other hand were collected from the damp rainy upland forest of Black River Gorges National Park at an altitude of about 709 meters above sea level and were therefore adapted to another environment.

3.1.2. Anatomy

The leaves of the three *Polyscias* species are hypostomatous with stomata irregularly scattered throughout the abaxial epidermis (Figure 3). This type of stomatal patterning observed is quite common in broad-leaved eudicots. Amphistomaty has been reported to occur mostly in fast-growing herbaceous annuals and slow-growing perennial shrubs and trees (Harrison et al., 2020).

The estimated stomatal density and length of closed stomata for PD, PG, and PM were 151, 85, and 282 stomata per mm^2, and 26.3, 33.3, and 22.9 µm, respectively. PG leaves had the greatest pore size while their stomatal density was considerably lower than the other two species. The PM tree is adapted to a damp and rainy environment and its leaves had the highest stomatal density.

Though the overall shape of stomata is genetically pre-determined, their development is influenced by environmental conditions (Harrison et al., 2020; Driesen et al., 2020). Plants with large and few stomata tend to have higher water-use efficiency as compared with plants that have many but smaller stomata (Drake et al., 2013). It has been reported that small stomatal size can provide a reduction in total leaf pore area and may facilitate faster aperture response than large stomata (Bertolino et al., 2019).

Figure 2. Leaves and leaflets of: A-PD; B-PG; C-PM (Bar = 2 cm)

3.1.3. Transverse sections of leaves

The leaflets of the three species are of the dorsiventral type and have several layers of hypodermal collenchyma on the upper and lower side of the midrib region. Vascular bundles in the midrib are collateral and the xylem tissue is endarch. Several secretory cavities are circularly arranged in the peripheral region of the midrib. The epidermis on both the abaxial and adaxial sides of the lamina are multiseriate and covered with a cuticular layer. Their upper epidermis is four-layered thick while their lower epidermis is two-layered thick. Palisade mesophyll composed of two layers of elongated columnar cells is found below the upper epidermis and spongy mesophyll is situated just above the lower epidermis. Several vascular bundles are centrally located in the leaf lamina.

The leaf anatomy of the three species differs in many ways. In the midrib region of PD leaflets, the vascular tissues are arranged in an arc-shaped belt with two patches just inside the two ends (Figure 4 A). In PG (Figure 4 B) and PM (Figure 4 C), vascular bundles are arranged in a semicircle, though in PM, several vascular bundles are scattered within the semicircle in the central region of their midrib. Furthermore, the spongy mesophyll of PD and PM is made up of loosely arranged cells with intercellular spaces, while that of PG is relatively compact.

The shape of the midrib was different in the three species (Figure 4). The thickness of the midrib and lamina of PD, PG, and PM leaflets were approximately 0.97, 0.96, and 2.1 mm, and 0.44, 0.37, and 0.20 mm, respectively. The thickness of the midrib of the PM leaflets was approximately twice that of the other two *Polycias* species while its lamina was about half their thickness. The diameters of whole veins can reflect their transport capacity and the degree of mechanical support (Sack and Scoffoni, 2013). The thickness of the lamina largely determines the length of the optical path of light through a leaf and is associated with water deficits, low temperature, and high irradiance (Pauli et al., 2017).

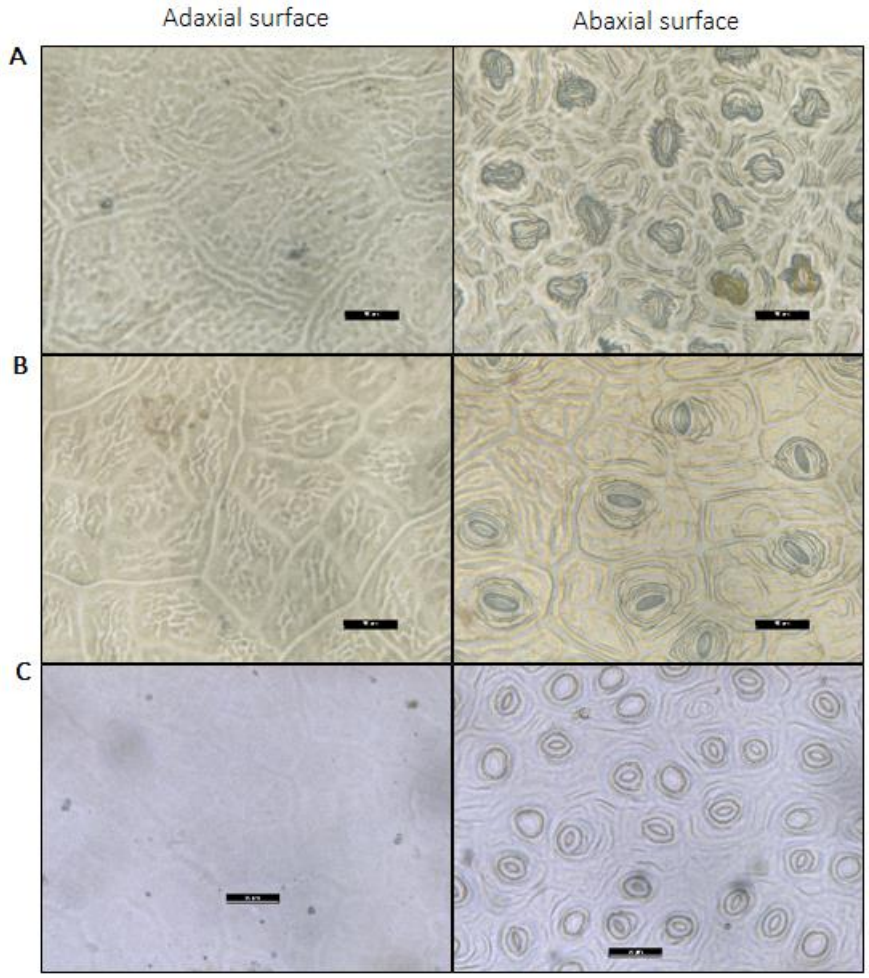

Figure 3. Adaxial surface and abaxial surface with guard cells of leaf blade of: A-PD; B-PG; C-PM (Bar = 50 µm)

3.2. Chemical profiling

The presence of the terpenes and terpenoids were identified in hexane and ethanol extracts of the three species using TLC and test tube testing. Flavonoids in ethanol and aqueous extracts, sterols in aqueous extracts, and saponins were detected in all the extracts. No alkaloids were present in the different extracts.

The NMR spectra of three extracts of air-dried leaves of *Polyscias* spp. showed a difference in chemical signals suggesting the presence of different metabolites in each extract (Figures S1-S6/supplementary file).

In the ^{1}H NMR spectra of the hexane extracts, the major signals were in the region of δ 0.3 to 3.0 and δ 5.1 to 5.6 ppm which were attributed to aliphatic and olefinic protons, respectively. In ^{13}C NMR spectra, the signals in the region of 10 to 60 ppm corresponded to sp^3 hybridized $CH_3/CH_2/CH$ while those in the region of 110 to 120 ppm were due to olefinic carbons. These data indicated mainly the presence of terpenes in the hexane extracts.

In the more polar ethanolic extracts, in addition to the signals due to terpenes moieties, signals in the region δ 3.5 to 5.0 ppm were attributed to sugar moieties. Signals in the region of δ 10 to 55 ppm corresponded to triterpenoid moiety while those in the region of 80 to 110 ppm indicated the presence of sugar moiety. The peaks in the region of 120 to 145 ppm corresponded to sp^2 carbons and the signal at δ 173 ppm were due to the ester group. These data indicated the presence of different terpene/terpenoid saponins and flavonoids in the extracts.

The ^{1}H NMR spectra of the aqueous extracts showed signals at δ 0.8 to 2.7 ppm for aliphatic protons and the more downfield signals (δ 3 to 4 ppm) were attributed to tertiary and allylic methyl groups attached to hydroxyl moiety. These data suggest the presence of steroids in the aqueous extracts.

The different metabolites from the leaf extracts of the PG, PD, and PM were identified using LC-MS/MS. The chemical structure of the phytochemicals was confirmed by the comparison with the literature value and molecular/fragment ions from positive and negative ion modes. It is important to note that this paper does not give the complete structural identification of different species identified in the various extracts.

From the different *Polyscias* species, a total of 31 triterpenoid saponins, 19 flavonoids, 17 derivatives of acids, 7 terpenes, and 10 miscellaneous compounds including pyrrolidines, acetylenes, and sterols were identified. The molecular formula, mass, and fragment ions are given in Table 1.

LC-MS/MS allowed the identification of major saponins and aglycones. The major class of compounds is triterpenoids saponins which consist of a triterpene aglycone with 30 carbon atoms with

one or more sugar moieties (including hexoses, pentoses, methylhexoses). Twenty-one triterpenoid saponins were identified in the negative ion mode while ten were detected in the positive ion mode. Through the relationship of deprotonated ions of triterpenoid saponins, 648-1294 and the protonated *m/z* 620-1220, four aglycones with a molecular weight of 456, 471, 466, and 485 (Figure 5) were detected as daughter ions. The molecular formula of the aglycones was deduced by the loss of sugar molecules from the respective parent ions. Oleanolic acid and hederagenin are the major aglycones while glucose (Glu), glucuronic acid (GluA), glucuronic methyl ester (MeGluA), rhamnose (Rha), methyl pentose (Mepen) and arabinose (Arab) are the main sugar moieties. These sugar molecules were identified by the presence of molecular fragments corresponding to *m/z* 163, 177, 191, 147, 146, and 133.

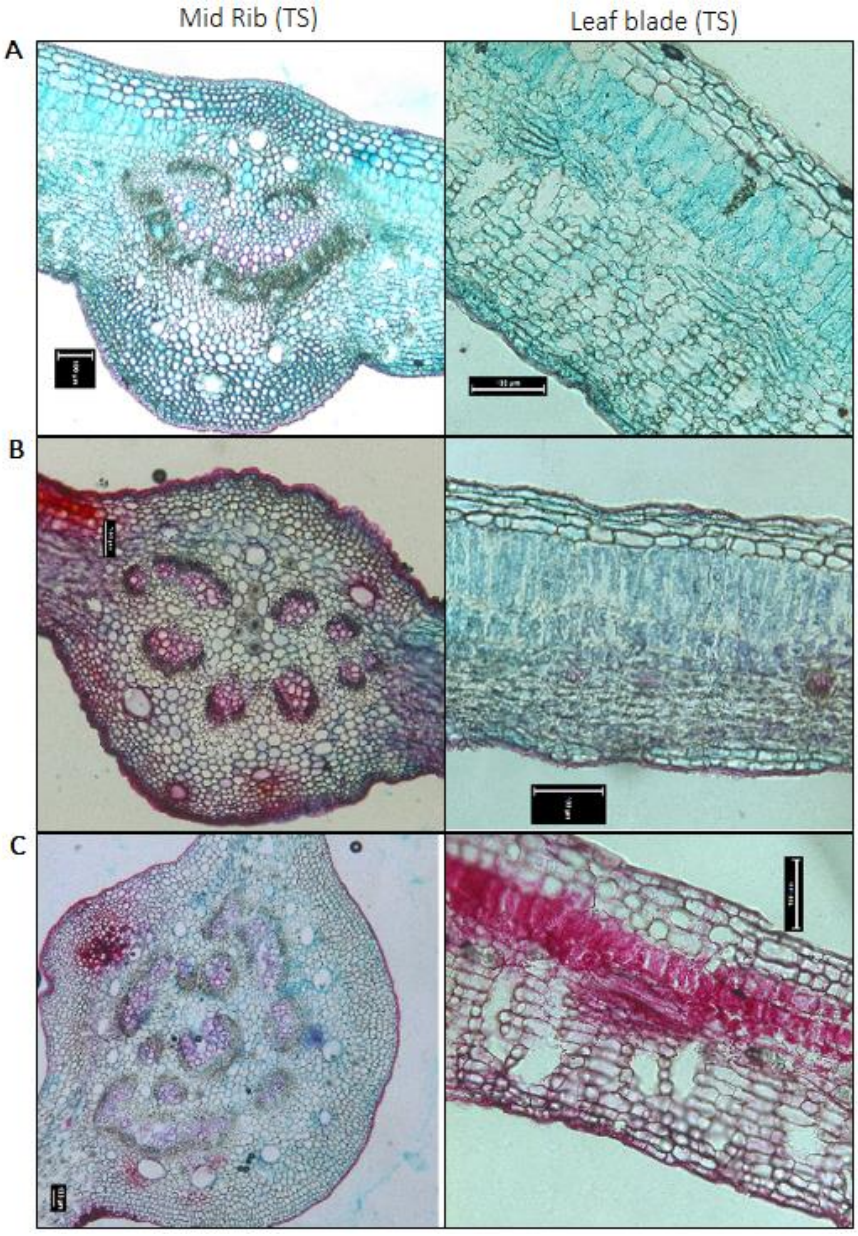

Figure 4. Leaf transverse sections showing the midrib and leaf blade of: A-PD; B-PG; C-PM (Bar = 100 µm)

Flavonoids are fifteen-carbon skeletons consisting of two benzene rings linked via a heterocyclic pyrene ring and may contain glycosides. The main flavonoid aglycones are kaempferol and quercetin containing one and two sugar moieties. Two flavones, namely acacetin, and vitexin (F1, F7) and catechin (F3) and its methoxy derivative (F5) were identified using fragmentation patterns in mass spectra. The two main flavonols kaempferol (F2), quercetin (F4), and their methoxy derivatives (tamarixetin, F6) containing one to four sugar moieties were detected (Figure 6) (Table 1).

The presence of the fragment ion *m/z* 191 in the mass spectra of the six acids (A8, A10, A11, A13, A15, A16) showed them to be quinic acid derivatives. A9, A12, and A14 were identified as acid glycosides based on the loss of sugar moieties from the parent ion (Table 2). Two pyrrolidine derivatives containing carboxylic acid and hydroxyl ethyl residue were detected. Steroid derivatives namely ergosterol, campestanol, and sitosterol were also identified (Table 2).

3.3. Biological properties

3.3.1. Antibacterial activity

Plant constituents such as flavonoids, terpenes, alkaloids, and tannins are known to display antibacterial activity (Tankeo et al., 2015). The different leaf extracts exhibited moderate inhibition (8-10 mm) at the concentration of 400 mg/ml against a set of gram-positive and gram-negative bacteria. The hexane extracts of the different species showed the highest inhibitory activity which may be attributed to the presence of several terpenes. The ethanolic extract containing several saponins was found to exhibit moderate activity in line with Maritim (Winnie et al., 2019).

Table 1. Triterpenoids and flavanoids detected from the leaves extract of *Polyscias* spp.

Compound	Formula	m/z	$[M-H]^-$ m/z	$[M+H]^+$ m/z	MS/MS	PG			PD			PM			Reference
						Hex	EtOH	Aq	Hex	EtOH	Aq	Hex	EtOH	Aq	
TS1	$C_{30}H_{48}O_4$	472		473	463, 350, 301, 293		+		+	+	+				(Mitaine-Offer et al., 2004)
TS2	$C_{32}H_{49}O_3$	480		481	467, 425, 409, 305, 191			+							(Masruri et al., 2007)
TS3	$C_{35}H_{56}O_9$	620		621	620, 474, 424, 402		+								(Eaton et al., 2015)
TS4	$C_{37}H_{56}O_8$	628		629	509,482,467,425,403	+	+								(Masruri et al., 2007)
TS5	$C_{36}H_{58}O_{10}$	648	647		603, 471			+		+			+		*
TS6	$C_{37}H_{58}O_{10}$	662	661		570, 602,615			+							*
TS7	$C_{41}H_{66}O_{12}$	750	749	751	471, 585, 603, 749			+					+		(Winnie et al., 2019)
TS8	$C_{41}H_{66}O_{13}$	766		767	739, 585, 455, 437								+		(Ashmawya et al., 2020)
TS9	$C_{42}H_{68}O_{13}$	780	779		455, 732	+	+						+		(Masruri et al., 2007)
TS10	$C_{41}H_{65}O_{14}$	781		782	471, 453					+					(Huan et al., 1998)
TS11	$C_{42}H_{66}O_{14}$	794	793		473, 585, 602, 747	+	+			+	+	+	+		(Paphassarang et al., 1989)
TS12	$C_{42}H_{68}O_{14}$	796	795		601, 471	+						+		+	*
TS13	$C_{43}H_{68}O_{14}$	808	807		495, 591			+							(Sugimoto et al., 2017; Elgindi et al., 2015)
TS14	$C_{42}H_{68}O_{15}$	810	809		485, 617, 765		+			+					(Nascimento et al., 2019)
TS15	$C_{42}H_{68}O_{15}$	810		811	765, 603, 471		+		+	+					*
TS16	$C_{44}H_{72}O_{14}$	824	823		577, 603, 739, 777		+	+					+		(Elgindi et al., 2015)
TS17	$C_{44}H_{72}O_{14}$	824	823		455			+							*
TS18	$C_{44}H_{69}O_{15}$	837	836		225, 340, 452, 564, 772, 790	+			+			+			*
TS19	$C_{43}H_{66}O_{16}$	838	839		471			+							*
TS20	$C_{48}H_{77}O_{17}$	925		924	762, 601, 583, 565, 471, 455, 437, 309								+		(Nascimento et al., 2019)
TS21	$C_{48}H_{78}O_{18}$	942		943	455, 437, 408, 309								+		(Paphassarang et al., 1990)
TS22	$C_{49}H_{78}O_{19}$	970	969		247, 441, 453			+					+		(Do et al., 2020)
TS23	$C_{48}H_{76}O_{20}$	972	973		603, 323								+		(Elgindi et al., 2015)
TS24	$C_{48}H_{75}O_{21}$	986		987	453, 471		+		+					+	*
TS25	$C_{48}H_{74}O_{21}$	986	985		457, 469			+					+		*
TS26	$C_{54}H_{88}O_{24}$	1120	1119		471, 585, 603, 749			+		+			+		(Hanh et al., 2016)
TS27	$C_{59}H_{96}O_{26}$	1220		1221	455, 437, 409, 293		+	+					+		(Njateng et al., 2017)
TS28	$C_{60}H_{98}O_{27}$	1250	1249		255, 731		+								(Huan et al., 1998)
TS29	$C_{60}H_{98}O_{28}$	1266	1265		205, 247, 469, 749	+	+	+					+		(Huan et al., 1998)
TS30	$C_{60}H_{97}O_{29}$	1282	1281		603, 465, 362					+					(Hanh et al., 2016)
TS31	$C_{60}H_{94}O_{30}$	1294	1293		258, 453, 746, 777		+								*
F1	$C_{16}H_{12}O_5$	284		285	240									+	(Lin et al., 2019)
F2	$C_{15}H_{10}O_6$	286		287	270, 226, 106	+	+	+	+		+				*
F3	$C_{15}H_{14}O_6$	290	289		146, 174		+						+		(Li and Seeram, 2018)
F4	$C_{15}H_{10}O_7$	302		303	282, 109		+	+	+	+	+				(Figat et al., 2020)
F5	$C_{16}H_{16}O_6$	304	303		266, 248, 175, 147, 134				+	+					*
F6	$C_{16}H_{12}O_7$	316		317	298, 254, 106	+	+	+			+		+		(Sugimoto et al., 2017)

Compound	Formula	m/z	$[M-H]^-$ m/z	$[M+H]^+$ m/z	MS/MS	PG			PD			PM			Reference
						Hex	EtOH	Aq	Hex	EtOH	Aq	Hex	EtOH	Aq	
F7	$C_{21}H_{20}O_{10}$	432	431		153, 205			+		+			+		(Li and Seeram, 2018)
F8	$C_{21}H_{20}O_{11}$	448	447		161, 269, 398		+	+		+			+	+	(Eaton et al., 2015; Elgindi et al., 2015; Lin et al., 2019)
F9	$C_{21}H_{20}O_{12}$	464	463	465	254, 271, 300			+					+		(Bedir et al., 2001)
F10	$C_{21}H_{18}O_{13}$	478	477		151, 179, 301		+	+					+	+	*
F11	$C_{27}H_{30}O_{15}$	594	593		207	+									(Ashmawya et al., 2019)
F12	$C_{28}H_{32}O_{15}$	608		609	591, 577, 559, 531, 515, 475				+	+					(Sugimoto et al., 2017)
F13	$C_{27}H_{30}O_{16}$	611	610		564, 543, 450				+	+					(Figat et al., 2020)
F14	$C_{28}H_{32}O_{16}$	624	625		607, 565, 538, 521, 465, 477				+	+	+				*
F15	$C_{27}H_{30}O_{17}$	626	627		607, 565, 538,521, 465										*
F16	$C_{23}H_{40}O_{20}$	636		637	619, 587, 559, 476	+		+							*
F17	$C_{30}H_{32}O_{19}$	696		697	311						+				*
F18	$C_{33}H_{40}O_{20}$	757		758	283					+					*
F19	$C_{39}H_{52}O_{25}$	920		921	627, 609, 591, 331		+		+						*

*Based on mass fragments

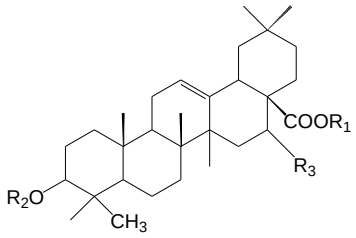

TS8: R_1= H, R_2= Arab-Glu, R_3=OH
TS9: R_1= H, R_2= Glu-Glu, R_3=H
TS10: R_1= H, R_2= GluA-Arab, R_3=OH
TS11: R_1= H, R_2= GluA-Rham, R_3=OH
TS13: R_1= Glu, R_2= MeGluA, R_3=H`
TS17: R_1= H, R_2= MegluA -Glu, R_3=OH
TS18: R1= H, R2= MegluA - MegluA, R_3=H
TS20: R_1= Ara, R_2= MegluA-Arab, R_3=OH
TS21: R_1= Glu, R_2= Glu-Glu, R_3=H
TS22: R_1= Glu, R_2= MeGluA-Glu, R_3=H
TS24: R_1= GluA, R_2= GluA-Glu, R_3=OH
TS26: R_1= Glu, R_2= Glu-Glu-Glu, R_3=OH
TS27: R_1= Rham-Glu-Glu, R_2= Rha-Ara, R_3=OH
TS28: R_1= Glu-Rha, R_2= Glu-Glu-Glu, R_3=H
TS30: R_1= Glu-Glu, R_2= GluA(Glu)-Glu, R_3=H
TS31: R_1= GluA-Glu, R_2= GluA(Glu)-Glu, R_3=H

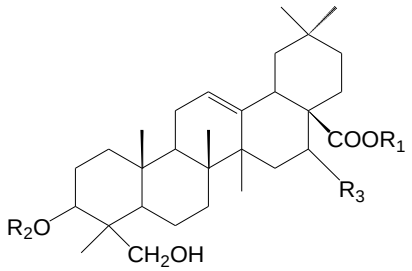

TS1: R_1= H, R_2=H, R_3= H
TS3: R_1= H, R_2=Ara, R_3= OH
TS5: R_1= H, R_2=GluA, R_3= H
TS6: R_1= H, R_2=MeGluA, R_3= H
TS7: R_1= H, R_2=Arab-Rham, R_3= H
TS12: R_1= H, R_2=Glu-Glu, R_3= H
TS15: R_1= H, R_2= Arab-MeGluA, R_3=OH
TS16: R_1= H, R_2= MeGluA-Glu, R_3=H
TS19: R_1= H, R_2= MeGluA-GluA, R_3=H
TS29: R_1= Glu-Rha, R_2= Glu-Glu-Glu, R_3=H

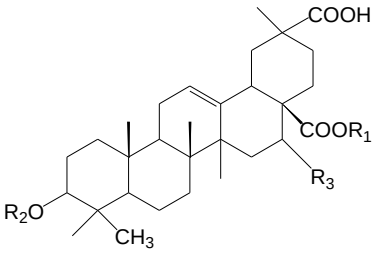

TS14: R_1= Glu, R_2=Glu
TS23: R_1= H, R_2= MegluA-Glu-Ara
TS25: R_1= Glu, R_2= GluA-Glu

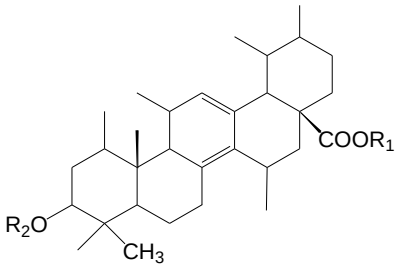

TS2: R_1= CH3, R_2=H
TS4: R_1= Glu, R_2=H

Figure 5. Proposed structures of triterpenoid saponins

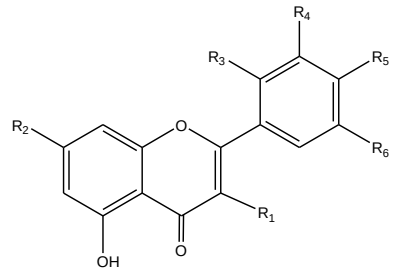

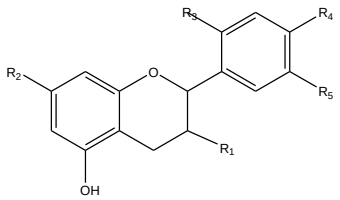

F2: R_1= OH; R_2= OH; R_3=H, R_4=H; R_5=OH; R_6=H
F4: R_1= OH; R_2= OH; R_3=H, R_4=OH; R_5=OH, R_6=H
F6: R_1= OH; R_2= OH; R_3=H, R_4=OH; R_5=OCH_3, R_6=H
F8: R_1= ORham; R_2= OH; R_3=H, R_4=OH; R_5=OH, R_6=H
F9: R_1= OGlu; R_2= OH; R_3=H, R_4=H; R_5=OH, R_6=OH
F10: R_1= OGluA; R_2= OH; R_3=H, R_4=OH; R_5=OH, R_6=H
F11: R_1= ORham; R_2= ORham; R_3=H, R_4=H; R_5=OH, R_6=OH
F12: R_1= ORham; R_2= ORham; R_3=H, R_4=H; R_5=OCH_3, R_6=OH
F13: R_1= OGlu-Rham; R_2= OH; R_3=OH, R_4=H; R_5=OH, R_6=OH
F14: R_1= OGlu; R_2= ORham; R_3=H, R_4=H; R_5=OCH_3, R_6=OH
F15: R_1= OGlu; R_2= OGlu; R_3=OH, R_4=H; R_5=OH, R_6=H
F16:R_1= ORham; R_2= OMegluA; R_3=H, R_4=H; R_5=OCH_3, R_6=H
F17: R_1= OMegluA; R_2= OMegluA; R_3=H, R_4=H; R_5=OCH_3, R_6=OH
F18: R_1= OGlu-Rham; R_2= ORham; R_3=OH, R_4=H; R_5=OH, R_6=H
F19: R_1= OGlu-Rham; R_2= OGlu-Rham; R_3=OH, R_4=H; R_5=OH, R_6=H

F3:R_1=OH; R_2= OH; R_3=H, R_4=OH, R_5=OH
F5:R_1=OH; R_2= OCH_3; R_3=H, R_4=OH, R_5=OH

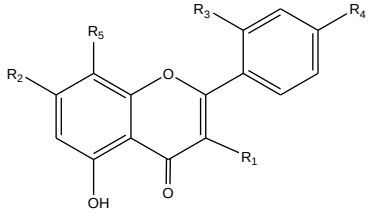

F1:R_1= H; R_2= OH; R_3=H, R_4=OCH_3, R_5=H
F7: R_1= H; R_2=OH; R_3=H, R_4=OH; R_5=Glu

Figure 6. Proposed structure of flavanoids

Table 2. Proposed structure of acids, terpenes and miscellaneous compounds detected in the extracts of *Polyscias* spp.

Identified compounds		m/z	$[M-H]^-$	$[M+H]^+$	MS	PG			PD			PM			Reference
Name/Formula			m/z	m/z		Hex	EtOH	Aq	Hex	EtOH	Aq	Hex	EtOH	Aq	
Acids															
A1	Malic Acid ($C_4H_6O_5$)	134	133		115	+	+	+			+	+		+	(Figat et al., 2020)
A2	Procatechuic acid ($C_7H_6O_4$)	154	153		109	+	+	+						+	(Lin et al., 2019)
A3	3-(4-Hydroxyphenyl) propionic acid ($C_9H_{10}O_3$)	166	165		121	+						+			(Ashmawy a et al., 2020)
A4	Caffeic acid ($C_9H_8O_4$)	180	179		115, 132, 163	+									(Lin et al., 2019)
A5	Quinic acid ($C_7H_{12}O_6$)	192	191		111, 129		+	+			+			+	(Willems et al., 2016)
A6	Methyl 2,4-dihydroxy-3,6-dimethylbenzoate (Atraric acid) ($C_{10}H_{12}O_4$)	196	195	197	160, 135, 114				+	+				+	(Willems et al., 2016)
A7	Hydroxy-octadecatrienoic acid ($C_{18}H_{30}O_3$)	294	293		236, 220, 221, 218, 194	+	+	+		+		+	+		(Figat et al., 2020)
A8	5-*O*-Caeffoylquinic acid ($C_{16}H_{18}O_8$)	338	337		172, 191		+	+					+		(Willems et al., 2016)
A9	Caeffeoyl glucose ($C_{15}H_{18}O_9$)	342	341	343	135, 161, 179, 221, 251	+	+	+		+	+		+		(Said et al., 2017)
A10	5-*O*-Caffeoylquinic acid (chlorogenic acid) ($C_{16}H_{18}O_9$)	354	353		179, 191	+	+	+					+	+	*
A11	5-*O*-Feruloyquinic acid ($C_{17}H_{20}O_9$)	368	367		191	+	+	+					+	+	*
A12	Caffeoyl-glucaric acid ($C_{15}H_{16}O_{11}$)	372	371		191, 209	+									*
A13	Quinic acid derivative	407	406		282, 190, 161, 135						+				*
A14	Procatechuic acid containing glucose and gluconic ($C_{25}H_{32}O_{10}$)	492		490/491/494	467, 425, 407, 177, 163			+	+	+					*
A15	3,5-di-*O*-caffeoyl-quinic acid ($C_{25}H_{24}O_{12}$)	516	515		179, 191	+	+	+		+			+	+	(Figat et al., 2020)
A16	Quinic acid derivative	548	547		134, 149, 191			+							*

Identified compounds		m/z	$[M-H]^-$	$[M+H]^+$	MS	PG			PD			PM			Reference
Name/Formula			m/z	m/z		Hex	EtOH	Aq	Hex	EtOH	Aq	Hex	EtOH	Aq	
A17	Phenolic acid derivative	584	583		195, 534		+								(Sliwinska et al., 2018)
Terpenes															
T1	Terpene ($C_{15}H_{18}$)	198		199	178, 159, 156, 148, 137	+									(Ashmawy a et al., 2018)
T2	Sesquiterpene ($C_{15}H_{24}$)	204		203	147, 121, 119, 109, 107				+	+					(Ashmawy a et al., 2018)
T3	Phytol ($C_20H_{40}O$)	296	295	297	185, 277	+	+			+					(Ashmawy a et al., 2018)
T4	Diterpenoid ($C_{20}H_{34}O_3$)	322		323				+							(Ashmawy a et al., 2020)
T5	Diterpenoid ($C_{20}H_{26}O_4$)	330		329	284, 106		+								(Tang et al., 2011)
T6	Diterpenoid ($C_{21}H_{30}O_4$)	346		347	240, 283, 106	+	+	+		+	+				*
T7	Squalene ($C_{30}H_{50}$)	410		411	239, 133		+								(Bertilino et al., 2019)
Others															
	5-Oxopyrrolidine-2-carboxylic acid ($C_5H_7NO_3$)	129		130	112		+								(Sugimoto et al., 2017)
	2-Hydroxyethyl 5-oxopyrrolidine-2-carboxylate ($C_7H_{11}NO_4$)	173		174	165, 163, 162, 153				+						(Sugimoto et al., 2017)
	Falcarinol ($C_{17}H_{24}O$)	244		243	241, 232, 223, 214, 133	+		+							(Ashmawy a et al., 2020)
	Heptadeca-1,8-diene-4,6-diyne-3-ol-10-one ($C_{17}H_{22}O_2$)	258		259				+	+			+			(Ashmawy a et al., 2020)
	Pinoresinol ($C_{20}H_{22}O_6$)	358		359	340, 312/ 350, 293, 237	+	+	+	+	+	+				(Njateng et al., 2017)
	Ergosterol ($C_{28}H_{44}O$)	396		397	379, 239, 229, 177, 133			+		+					(Münger et al., 2018)
	Campestanol ($C_{28}H_{50}O$)	402	401		121, 181, 223,312, 357		+	+							(Münger et al., 2018)
	Canthoside A ($C_{18}H_{26}O_{12}$)	434	433		227, 387		+								(Lin et al., 2019)
	β-sitosterol ($C_{29}H_{50}O$)	414	415		406, 350,307,293	+	+		+	+	+				(Ragasa et al., 2015)

*Based on mass fragments

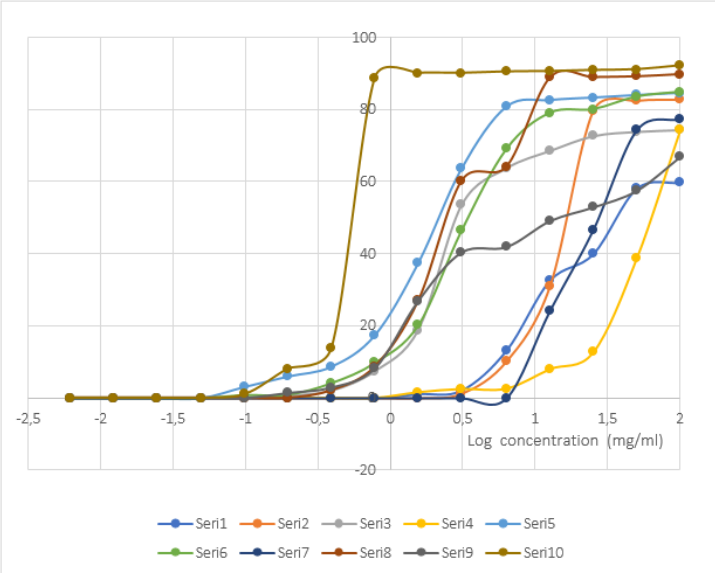

Figure 7. Percentage inhibition of different extracts of *Polyscias* spp.

Table 3. Radical scavenging activity SC_{50} (mg/ml) of the different extracts

Extracts	PM	Category	PG	Category	PD	Category
Hex	14.6	Weak	48.8	Weak	46.1	Weak
EtOH	2.3	Strong	7.4	Moderate	2.2	Strong
Aq	16.8	Moderate	4.6	Strong	3.2	Strong

Ascorbic acid SC_{50}: 0.6 mg/ml

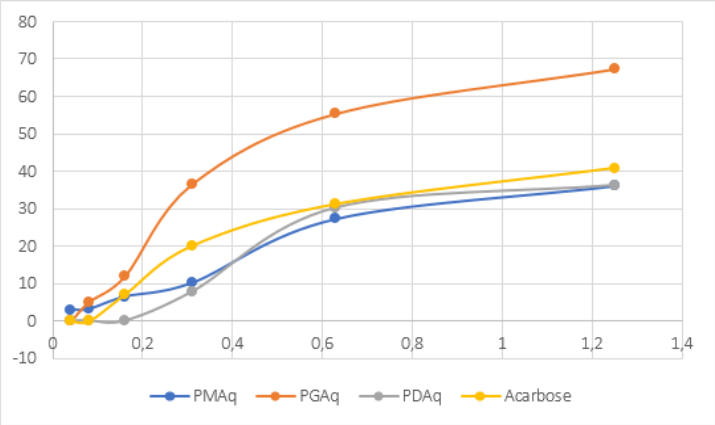

Figure 8. Anti-α-glucosidase activity of aqueous extract of *Polyscias* spp.

3.3.2. Antioxidant capacity

Extracts from the three species showed significant levels of radical scavenging activity and were dose-dependent (Figure 7) with IC_{50} values in the range of 2.1-70.8 mg/ml (Table 3). The ethanolic and aqueous extracts were found to be potent DPPH scavengers as compared to the hexane extracts. The presence of several flavonoids (including acacetin, kaempferol, catechin, and quercetin), glucosides derivatives, and quinic acid derivatives (Figure 5 and Table 1) contributes to their anti-oxidant activity (Njateng et al., 2017).

3.3.3. Anti-α-glucosidase activity

The inhibitory effects of the aqueous extracts were evaluated against yeast α-glucosidase with acarbose as the positive control. Pentacyclic triterpenoids saponins have been reported to exhibit α-amylase and α-glucosidase activity (Luyen et al., 2018). The presence of glucuronic acid and glucosidic moieties on the aglycones were essential components for α-glucosidase inhibition (Hanh et al., 2016). The extracts of PG and PM potently inhibited α-glucosidase with IC_{50} values of 0.50 and 2.62 mg/ml and were comparable to the acarbose with an IC_{50} value of 2.40 mg/ml (Figure 8).

4. Conclusions

The leaves of the three endemic *Polyscias* species can be discriminated based on the shape and arrangement of the vascular tissue of the midrib. The extracts of these leaves showed to exhibit promising antioxidant and anti-glucosidase activities. From the phytochemical analysis, it was found that the major components were triterpenoid saponins, flavonoids, and acids. It is possible that the presence of these metabolites could be responsible for the observed biological properties.

Acknowledgments

One of the authors expresses her gratitude to Ms. Ryta Anath-Jugessur and Ms. Yousrina Bholah for the technical support. The authors are grateful to Mr. Pynee Kersley, Ministry of Agro-Industry and Food Security for the collection of the leaf samples.

Conflict of interest

The authors confirm that there are no conflicts of interest.

Funding

This research did not receive any specific grant from funding agencies in the public, commercial, or not-for-profit sectors.

CRediT authorship contribution statement

Minu Gupta Bhowon: Conceptualization, Data curation, Investigation, Analysis, Writing, Reviewing & editing the manuscript
Lee Suan Chua: Resources, Investigation
Shobha Jawaheer: Methodology, Investigation, Analysis, Writing
Ayeshna D. Soodhowa: Investigation, Analysis
Sabina Jhaumeer Laulloo: Conceptualization, Data curation, Investigation, Analysis, Writing, Reviewing & editing the manuscript

ORCID Numbers of the Authors

M.G. Bhowon: 0000-0003-1942-6098
L.S. Chua: 0000-0003-2493-9963
S. Jawaheer: 0000-0002-6273-9113
A.D. Soodhowa: 0000-0001-5551-3901
S.J. Laulloo: 0000-0001-8841-9276

Supplementary File

The supplementary file accompanying this article is available at https://ijpbp.com/index.php/ijpbp/libraryFiles/downloadPublic/8.

References

Ashmawya, N.S., Gad, H.A., Al-Musayeib, N., El-Ahmady, S.H., Ashour, M.L., Singab, A.N. B., 2019. Phytoconstituents from *Polyscias guilfoylei* leaves with histamine-release inhibition activity. *Zeitschrift für Naturforschung C*, 74(5-6), 145-150.

Ashmawya, N.S., Gad, H.A., Ashour, M.L., El-Ahmady, S.H., Singab, A.N.B., 2020. The genus *Polyscias* (Araliaceae): A phytochemical and biological review. *Journal of Herbal Medicine*, 23, 100377.

Ashmawya, N.S., Gad, H.A., Ashoura, M.L., El-Ahmadya, S.H., Singab, A.N.B., 2018. Comparative study on the volatile constituents of *Polyscias guilfoylei* and *Polyscias balfouriana* leaves. *Medicinal & Aromatic Plants*, 7(6), 321.

Baider, C., Florens, F.V., Baret, S., Beaver, K., Matatiken, D., Strasberg, D., Kueffer, C., 2010. Status of plant conservation in oceanic islands of the Western Indian Ocean. In Proceedings of the 4th global botanic gardens congress (Vol. 2, pp. 1-7). Dublin: National Botanic Gardens of Ireland.

Bedir, E., Toyang, N.J., Khan, I.A., Walker, L.A., Clark, A.M., 2001. A new dammarane-type triterpene glycoside from *Polyscias fulva*. *Journal of Natural Products*, 64(1), 95-97.

Bertolino, L.T., Caine, R.S., Gray, J.E., 2019. Impact of stomatal density and morphology on water-use efficiency in a changing world. *Frontiers in Plant Science*, 10, 225.

Do, V.M., Tran, C.L., Nguyen, T.P., 2020. Polysciosides J and K, two new oleanane-type triterpenoid saponins from the leaves of *Polyscias fruticosa* (L.) harms. cultivating in An Giang Province, Viet Nam. *Natural Product Research*, 34(9), 1250-1255.

Drake, P.L., Froend, R.H., Franks, P.J., 2013. Smaller, faster stomata: scaling of stomatal size, rate of response, and stomatal conductance. *Journal of Experimental Botany*, 64(2), 495-505.

Driesen, E., Van den Ende, W., De Proft, M., Saeys, W., 2020. Influence of environmental factors light, CO_2, temperature, and relative humidity on stomatal opening and development: A review. *Agronomy*, 10(12), 1975-2002.

Eaton, A.L., Brodie, P.J., Callmander, M.W., Rakotondrajaona, R., Rakotobe, E., Rasamison, V.E., Kingston, D.G., 2015. Bioactive Oleanane Glycosides from *Polyscias duplicata* from the Madagascar Dry Forest. *Natural Product Communications*, 10(4), 567-570.

Elgindi, M.R., Melek, F.R., Hassan, M.A., Abdelaziz, H.S., 2015. Saponins isolated from *Polyscias guilfoylei* F. Araliaceae. *Research Journal of Pharmaceutical, Biological and Chemical Sciences*, 6(3), 545–549.

Figat, R., Śliwińska, A., Stochmal, A., Soluch, A., Sobczak, M., Zgadzaj, A., Pietrosiuk, A., 2020. Antigenotoxic, anti-photogenotoxic, and antioxidant properties of *Polyscias filicifolia* shoots cultivated *in vitro*. *Molecules*, 25(5), 1090.

Fritz, M.A., Rosa, S., Sicard, A., 2018. Mechanisms underlying the environmentally induced plasticity of leaf morphology. *Frontiers in Genetics*, 9, 478.

Gopalsamy, N., Gueho, J., Julien, H.R., Owadally, A.W., Hostettmann, K., 1990. Molluscicidal saponins of *Polyscias dichroostachya*. *Phytochemistry*, 29(3), 793-795.

Hanh, T.T.H., Dang, N.H., Dat, N.T., 2016. α-Amylase and α-glucosidase inhibitory saponins from *Polyscias fruticosa* leaves. *Journal of Chemistry*, 2016, 2082946.

Harris, J.G., Harris, M.W., 1994. Plant identification terminology: an illustrated glossary (No. QK9 H37 2001). Utah: Spring Lake Publishing.

Harrison, E.L., Arce Cubas, L., Gray, J.E., Hepworth, C., 2020. The influence of stomatal morphology and distribution on photosynthetic gas exchange. *The Plant Journal*, 101(4), 768-779.

Huan, V.D., Yamamura, S., Ohtani, K., Kasai, R., Yamasaki, K., Nham, N.T., Chau, H.M., 1998. Oleanane saponins from *Polyscias fruticosa*. *Phytochemistry*, 47(3), 451-457.

Joondan, N., Laulloo, S.J., Caumul, P., Kharkar, P.S., 2019. Antioxidant, antidiabetic and anticancer activities of L-Phenylalanine and L-Tyrosine ester surfactants: *in vitro* and *in silico* studies of their interactions with macromolecules as plausible mode of action for their biological properties. *Current Bioactive Compounds*, 15(6), 610-622.

Laulloo, S.J., Bhowon, M.G., Soyfoo, S., Chua, L.S., 2018. Nutritional and biological evaluation of leaves of *Mangifera indica* from Mauritius. *Journal of Chemistry*, 2018, 1-9.

Li, C., Seeram, N.P., 2018. Ultra-fast liquid chromatography coupled with electrospray ionization time-of-flight mass spectrometry for the rapid phenolic profiling of red maple (*Acer rubrum*) leaves. *Journal of Separation Science*, 41(11), 2331-2346.

Lin, M., Han, P., Li, Y., Wang, W., Lai, D., Zhou, L., 2019. Quinoa secondary metabolites and their biological activities or functions. *Molecules*, 24(13), 2512.

Luyen, N.T., Dang, N.H., Binh, P.T.X., Hai, N.T., Dat, N.T., 2018. Hypoglycemic property of triterpenoid saponin PFS isolated from *Polyscias fruticosa* leaves. *Anais da Academia Brasileira de Ciências*, 90, 2881-2886.

Masruri, E., Elvina, D.I., Kristianingsih, E.P.U., Rahman, M.F., Rurini, R., 2007. Indentification of triterpenoid compound from *Polyscias fruticosa* Harms (Araliaceae) root bark. *In International Conference on Chemical Sciences*, Yogyakarta- Indonesia, 24-26 May.

Mitaine-Offer, A.C., Tapondjou, L.A., Lontsi, D., Sondengam, B.L., Choudhary, M.I., Lacaille-Dubois, M.A., 2004. Constituents isolated from *Polyscias fulva*. *Biochemical Systematics and Ecology*, 6(32), 607-610.

Münger, L.H., Boulos, S., Nyström, L., 2018. UPLC-MS/MS based identification of dietary steryl glucosides by investigation of corresponding free sterols. *Frontiers in Chemistry*, 6, 342.

Nascimento, Y.M., Abreu, L.S., Lima, R.L., Costa, V.C.O., Melo, J.I.M.D., Braz-Filho, R., Tavares, J.F., 2019. Rapid characterization of triterpene saponins from *Zornia brasiliensis* by HPLC-ESI-MS/MS. *Molecules*, 24(14), 2519.

Njateng, G.S.S., Du, Z., Gatsing, D., Mouokeu, R.S., Liu, Y., Zang, H.X., Kuiate, J.R., 2017. Antibacterial and antioxidant properties of crude extract, fractions and compounds from the stem bark of *Polyscias fulva* Hiern (Araliaceae). *BMC Complementary and Alternative Medicine*, 17(1), 99.

Paphassarang, S., Raynaud, J., Lussignol, M., Becchi, M., 1989. Triterpenic glycosides from *Polyscias scutellaria*. Phytochemistry, 28(5), 1539-1541.

Paphassarang, S., Raynaud, J., Lussignol, M., Cabalion, P., 1990. A new oleanolic glycoside from *Polyscias scutellaria*. *Journal of Natural Products*, 53(1), 163-166.

Pauli, D., White, J.W., Andrade-Sanchez, P., Conley, M.M., Heun, J., Thorp, K.R., Gore, M.A., 2017. Investigation of the influence of leaf thickness on canopy reflectance and physiological traits in upland and Pima cotton populations. *Frontiers in Plant Science*, 8, 1405.

Ragasa, C.Y., Ebajo, V.D., De Los Reyes, M.M., Brkljaca, R., Urban, S., 2015. Chemical constituents of *Polyscias nodosa*. *Research Journal of Pharmaceutical, Biological and Chemical Sciences*, 6(5), 1210-1214.

Rummun, N., Neergheen-Bhujun, V.S., Pynee, K.B., Baider, C., Bahorun, T., 2018. The role of endemic plants in Mauritian traditional medicine–Potential therapeutic benefits or placebo effect?. *Journal of Ethnopharmacology*, 213, 111-117.

Sack, L., Scoffoni, C., 2013. Leaf venation: structure, function, development, evolution, ecology and applications in the past, present and future. *New Phytologist*, 198(4), 983-1000.

Said, B.R., Arafa, I.H., Usam A,M., Abdullah Sulaiman, A.A., Kowalczyk, M., Moldoch, J., Stochmal, A., 2017. Tentative characterization of polyphenolic compounds in the male flowers of *Phoenix dactylifera* by liquid chromatography coupled with mass spectrometry and DFT. *International Journal of Molecular Sciences*, 18(3), 512.

Sliwinska, A.A., Syklowska-Baranek, K., Kosmider, A., Granica, S., Miszczak, K., Nowicka, G., Pietrosiuk, A., 2018. Stimulation of phenolic compounds production in the *in vitro* cultivated *Polyscias filicifolia* Bailey shoots and evaluation of the antioxidant and cytotoxic potential of plant extracts. *Acta Societatis Botanicorum Poloniae*, 87(2), 1-16.

Stasolla, C., Yeung, E.C., 2015. 'Paraffin and Polyester Waxes' in Edward Chee Tak Yeung, Claudio Stasolla, Michael John Sumner and Bing Quan Huang, eds. Plant Microtechniques and Protocols. Cham Springer International Publishing, pp. 45-66.

Sugimoto, S., Yamano, Y., Khalil, H.E., Otsuka, H., Kamel, M.S., Matsunami, K., 2017. Chemical structures of constituents from the leaves of *Polyscias balfouriana*. *Journal of Natural Medicines*, 71(3), 558-563.

Świątek, Ł., Sieniawska, E., Mahomoodally, M.F., Sadeer, N.B., Wojtanowski, K.K., Rajtar, B., Zengin, G., 2021. Phytochemical Profile and Biological Activities of the Extracts from Two *Oenanthe* Species (*O. aquatica* and *O. silaifolia*). *Pharmaceuticals*, 15(1), 50-61.

Tang, W., Harada, K., Kubo, M., Hioki, H., Fukuyama, Y., 2011. Eight new clerodane diterpenoids from the bark of *Ptychopetalum olacoides*. *Natural Product Communications*, 6(3), 327-332.

Tankeo, S.B., Tane, P., Kuete, V., 2015. *In vitro* antibacterial and antibiotic-potentiation activities of the methanol extracts from *Beilschmiedia acuta*, *Clausena anisata*, *Newbouldia laevis* and *Polyscias fulva* against multidrug-resistant Gram-negative bacteria. *BMC Complementary and Alternative Medicine*, 15(1), 412.

Willems, J.L., Khamis, M.M., Saeid, W.M., Purves, R.W., Katselis, G., Low, N.H., El-Aneed, A., 2016. Analysis of a series of chlorogenic acid isomers using differential ion mobility and tandem mass spectrometry. *Analytica Chimica Acta*, 933, 164-174.

Winnie, C.M., Isabel, N.W., Josphat, C.M., 2019. Antibacterial saponins from the leaves of *Polyscias fulva* (Araliaceae). *African Journal of Biotechnology*, 18(19), 390-398.

Reviewed by:

Mayker L. D. Miranda: Instituto Federal de Educação, Ciência e Tecnologia do Triângulo Mineiro, Uberlândia, MG, BRAZIL

Andria Agusta: RC for Pharmaceutical Ingredient and Traditional Medicine, National Research and Innovation Agency, Cibinong, West Java 16911, INDONESIA

Valbona Aliko: Department of Biology, Faculty of Natural Sciences, University of Tirana, Tirana, ALBANIA

Publisher's Note: All claims expressed in this article are solely those of the authors and do not necessarily represent those of their affiliated organizations, or those of the publisher, the editors and the reviewers. Any product that may be evaluated in this article, or claim that may be made by its manufacturer, is not guaranteed or endorsed by the publisher.